NJC

Accepted Manuscript

This is an *Accepted Manuscript*, which has been through the Royal Society of Chemistry peer review process and has been accepted for publication.

Accepted Manuscripts are published online shortly after acceptance, before technical editing, formatting and proof reading. Using this free service, authors can make their results available to the community, in citable form, before we publish the edited article. We will replace this *Accepted Manuscript* with the edited and formatted *Advance Article* as soon as it is available.

You can find more information about *Accepted Manuscripts* in the Information for Authors.

Please note that technical editing may introduce minor changes to the text and/or graphics, which may alter content. The journal's standard Terms & Conditions and the Ethical guidelines still apply. In no event shall the Royal Society of Chemistry be held responsible for any errors or omissions in this *Accepted Manuscript* or any consequences arising from the use of any information it contains.

ROYAL SOCIETY OF CHEMISTRY

www.rsc.org/njc

New Journal of Chemistry

RSCPublishing

ARTICLE

Synthesis and Characterization of New Heterometallic Cyanido Complexes Based on $[Co(CN)_6]^{3-}$ Building Block: Crystal Structure of $[Cu_2(N\text{-}bishydeten)_2Co(CN)_6].3H_2O$ having a strong antiferromagnetic exchange

Cite this: DOI: 10.1039/x0xx00000x

Received ooth January 2012,
Accepted ooth January 2012

DOI: 10.1039/x0xx00000x

www.rsc.org/

Şengül Aslan Korkmaz[a], Ahmet Karadağ[b*], Yusuf Yerli[c] and Mustafa Serkan Soylu[d]

A tetradentate *N*- and *O*- donor, *N*,*N*-bis(2-hydroxyethyl)-ethylenediamine, (*N-bishydeten*), has been employed to synthesize four new heterometallic cyanido complexes; $[Ni_2(N\text{-}bishydeten)_2Co(CN)_6].3H_2O$ (**C1**), $[Cu_2(N\text{-}bishydeten)_2Co(CN)_6].3H_2O$ (**C2**), $[Zn_2(N\text{-}bishydeten)_2Co(CN)_6].5H_2O$ (**C3**) and $K[Cd(N\text{-}bishydeten)Co(CN)_6].1.5H_2O$ (**C4**). Characterization of the complexes was performed using *IR*, *EPR* (for **C2**), thermal analysis and elemental analysis techniques. The crystal structure of **C2** has been determined by the X-ray single crystal diffraction technique. The asymmetric unit of **C2** consists of cyanido-bridged trinuclear Cu1Cu2Co3 units {-CN-Cu1(*N-bishydeten*)-μ-O-Cu2(*N-bishydeten*)-NC-Co3$(CN)_4$-CN-} and three water molecules. The water molecules are situated in the inter-fragment spaces. The $[Cu_2(N\text{-}bishydeten)_2]^{2+}$ cations are linked to the $[Co(CN)_6]^{3-}$ anions via two cyanido bridges to give a *1D* neutral zigzag chain. One of two *N-bishydeten* bridges five coordinated Cu1 and six coordinated Cu2 through η^1-O2 deprotonated and the charge of **C2** is counterbalanced by this η^1-O2. The *IR* spectrum of **C2** is quite different from other complexes, three υ(C≡N) absorption bands were observed due to different cyanido groups in its structure. The thermal decompositions of **C1-C4** process in multi stages. Variable temperature magnetic susceptibility measurement recorded in the range 10–300 K showed the presence of a strong antiferromagnetic exchange interaction in **C2** between Cu1 and Cu2 by η^1-O2.

Introduction

The use of heterometallic networks is increasing with the understanding of how monometallic coordination polymers can be constructed and of their properties [1]. In the past few years, therefore, there has been a growing progress in the design of heterometallic assemblies particularly based on cyanidometallate complexes with the aim to give supramolecular architectures and provide molecular based magnets [2]. The most outstanding and long-known examples of cyanido complexes are represented by the mixed-valence polymeric structure of Prussian blue analogues which is ferromagnetic with the T_C = 5.6 K. This type of cyanido complexes is under investigation in coordination and organometallic chemistry at present.

Cyanido-bridged heterometallic complexes derived from hexacyanidometallates $[M(CN)_6]^{n-}$ (M = Co, Fe, Cr, etc., transition metals) and coordinatively unsaturated transition metal ions provide a variety of magnetic materials with *3D* extended networks [3,4]. It is known that hexacyanidometallates are excellent building blocks to serve as the bridging moiety in a multidimensional structure with a second transition metal coordinated by a polydentate ligand [3,5-7]. And also, this building block can adopt different bridging modes from η^1-η^6 to form bimetallic assemblies of various *1D*, *2D* and *3D* networks with interesting structures showing novel magnetic properties [5]. The *3D* framework is formed when neighboring blocks are linked at their N end through a second metal [8].
The cyano ligand plays an important role in the design of low dimensional magnetic coordination polymers because it is a good super exchange pathway between the paramagnetic metal ions. This ligand has the ability to serve as bridging group between neighboring

metal centers, removing electron density from the metal linked at the C end, through a π back-bonding interaction, to increase the charge density on the end N that is the coordination site for the other metal. This process leads to the overlapping between the electron clouds of neighboring metal centers and to their spin coupling and, thereby, a magnetic ordering is established. This interaction supports the role of hexacyanidometallates as prototype of molecular magnets [9].

Considering that the magnetic interactions are mediated by $[Co(CN)_6]^{-3}$ anions, it is useful to investigate the magnetic properties of heterometallic cyanido-bridged complexes. The structural and magnetic properties of some complexes based on $[Co(CN)_6]^{-3}$ building blocks have been rarely investigated and reported [2-7,10-20] for a long time and systematic studies on a series of hexacyanidocobaltate complexes have not yet been carried out.

In our previous studies, we have reported the tetracyanidonickelate [21] and tetracyanidopalladate [22] complexes with *N-bishydeten* ligand (I). As a part of our continuing research on cyanido complexes, herein we described the synthesis and characterization of hexacyanidocobaltate complexes with *N-bishydeten*, $[Ni_2(N\text{-}bishydeten)_2Co(CN)_6].3H_2O$ (**C1**), $[Cu_2(N\text{-}bishydeten)_2Co(CN)_6].3H_2O$ (**C2**), $[Zn_2(N\text{-}bishydeten)_2Co(CN)_6].5H_2O$ (**C3**) and $K[Cd(N\text{-}bishydeten)Co(CN)_6].1.5H_2O$ (**C4**). We characterized with *IR* and *EPR* (for **C2**) spectroscopies, elemental, and thermal analyses the structures of the complexes. Also the crystal structure of **C2** and magnetic susceptibilities of **C1** and **C2** were determined. In the synthesized cyanido-bridged title complexes, as a difference, the *N-bishydeten* ligand acts as a bridging ligand to form the two-dimensional layers. Therefore, the *N-bishydeten* ligand shows a bridging character, which is rare in the literature [21-24].

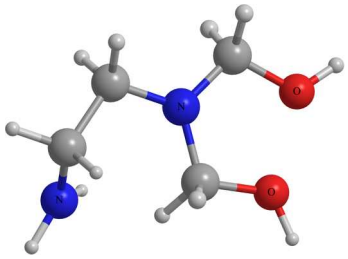

(I)

Experimental

Materials and instrumentation

$K_3[Co(CN)_6]$, $NiCl_2.6H_2O$, $CuCl_2.2H_2O$, $ZnCl_2$, $CdSO_4.8/3H_2O$ and *N-bishydeten* [*N*,*N*-bis(2-hydroxyethyl)-ethylenediamine ($C_6H_{16}N_2O_2$)] were obtained commercially and used without further purification.

Elemental analyses (C, H and N) were carried out using a LECO CHNS-932 elemental analyzer. IR spectra were measured in the 4000-400 cm^{-1} region with a Jasco 430 FT-IR Spectrometer in KBr pellets. The thermal analyses were performed on Perkin Elmer Diamond TG/DTA Thermal Analysis Instrument in nitrogen atmosphere with a heating rate of 3 or 10 $^oC\ min^{-1}$ and 5-10 mg sample. The 10-300 K magnetization measurements were carried out on a Quantum Design PPMS system. χ-T plots were recorded under the constant magnetic field of 5 kOe. Magnetic data were corrected for the diamagnetic contribution of the sample holder. The EPR powder spectrum was recorded with a Bruker EMX X-band spectrometer (9.8GHz) with about 20mW microwave power and 100 kHz magnetic field modulation.

Synthetic procedures

General procedure for synthesis of $[Ni_2(N\text{-}bishydeten)_2Co(CN)_6].3H_2O$ (C1)

An alcohol solution (15 ml) of *N-bishydeten* (2 mmol, 0.296 g), was added to a magnetically stirred solution of $NiCl_2.6H_2O$ (2 mmol, 0.476 g) in water (20 ml). The clear blue solution formed was added dropwise to a water solution (20 ml) of $K_3[Co(CN)_6]$ (1 mmol, 0.332 g) with stirring. After 5 min. a lilac precipitate formed. The product was filtered off, washed with water and dried in air. Yield: 83%. Anal. Cal. for $C_{18}H_{37}N_{10}O_7CoNi_2$; C, 31.71; H, 5.47; N, 20.54. Found: C, 31.82; H, 5.62; N, 21.44 %. IR (KBr disk, cm^{-1}) 3602, 3418 υ_{OH}; 3343, 3286 υ_{NH}; 2991, 2934, 2900, 2862 υ_{CH}; 2167, 2124 $\upsilon_{C\equiv N}$; 1616 δ_{OH}; 1459 δCH_2; 1218 υ_{CN}; 1065 υ_{CO}.

General procedure for synthesis of $[Cu_2(N\text{-}bishydeten)_2Co(CN)_6].3H_2O$ (C2)

The preparation of **C2** was carried out with a method similar to that of **C1**, except for use of $CuCl_2.2H_2O$ instead of $NiCl_2.6H_2O$. This solution was stirred until complete dissolution and after standing two weeks, dark blue polycrystalline solid was filtered off, washed with water and alcohol and then dried in air. Suitable crystals for X-ray analysis were obtained by slow evaporation of the solvent. Yield: 31%. Anal. Cal. for $C_{18}H_{37}N_{10}O_7CoCu_2$; C, 31.22; H, 5.53; N, 20.22. Found: C, 31.26; H, 5.16; N, 19.71%. IR (KBr disk, cm^{-1}) 3466-3144 υ_{OH} and υ_{NH}; 2992, 2965, 2932, 2895, 2871 υ_{CH}; 2172, 2152, 2135 $\upsilon_{C\equiv N}$; 1595 δ_{OH}; 1448 δCH_2; 1273 υ_{CN}; 1086 υ_{CO}.

General procedure for synthesis of $[Zn_2(N\text{-}bishydeten)_2Co(CN)_6].5H_2O$ (C3)

The **C3** was prepared in the same way as **C1** using $ZnCl_2$ (2 mmol, 0.272 g) instead of $NiCl_2.6H_2O$. Yield: 45%. Anal. Cal. for $C_{18}H_{41}N_{10}O_9CoZn_2$; C, 29.56; H, 5.65; N, 19.15. Found: C, 30.03; H, 5.79; N, 18.99 %. IR (KBr disk, cm^{-1}) 3506-3171 υ_{OH} and υ_{NH}; 2967, 2910, 2868 υ_{CH}; 2155, 2132 $\upsilon_{C\equiv N}$; 1622 δ_{OH}; 1453 δCH_2; 1283 υ_{CN}; 1061 υ_{CO}.

General procedure for synthesis of $K[Cd(N\text{-}bishydeten)Co(CN)_6].1.5H_2O$ (C4)

The white precipitate of **C4** was prepared in the same way as that of **C1** by using *N-bishydeten* (1 mmol, 0.148 g), $CdSO_4.8/3H_2O$ (1 mmol, 0.256 g) and $K_3[Co(CN)_6]$ (1 mmol, 0.332 g) at room temperature. Yield: 36%. Anal. Cal. for $C_{12}H_{19}N_8O_{3.5}KCoCd$; C, 26.60; H, 3.53; N, 20.68. Found: C, 26.48; H, 3.20; N, 21.39 %. IR (KBr disk, cm^{-1}) 3425, 3181 υ_{OH}; 3348, 3299 υ_{NH}; 2973, 2943, 2892, 2856 υ_{CH}; 2157 $\upsilon_{C\equiv N}$; 1604 δ_{OH}; 1462 δCH_2; 1242 υ_{CN}; 1019 υ_{CO}.

Crystallography

The air stable and prism blue single crystal of **C2** was selected with 0.47x0.34x0.27 mm dimensions and mounted in a STOE IPDS 2 diffractometer equipped with graphite monochromated Mo-K_α radiation (λ=0.71073 Å) at 293(2) K. The data collection and cell refinement were performed using STOE X-AREA [25] and STOE X-RED [25] was used for data reduction. The structures were solved by direct methods using SHELXS-97 [26] and non-hydrogen atoms were refined using full-matrix least-squares with anisotropic temperature factors (SHELXL-97) [26]. The coordinates of heavy

atoms were determined from direct methods and the positions of all non-hydrogen atoms were found by usual Fourier methods. The lattice parameters were determined by the least squares method on the basis of all reflections with F2>2(F2). The crystallographic data and other pertinent information are summarized in Table 1.

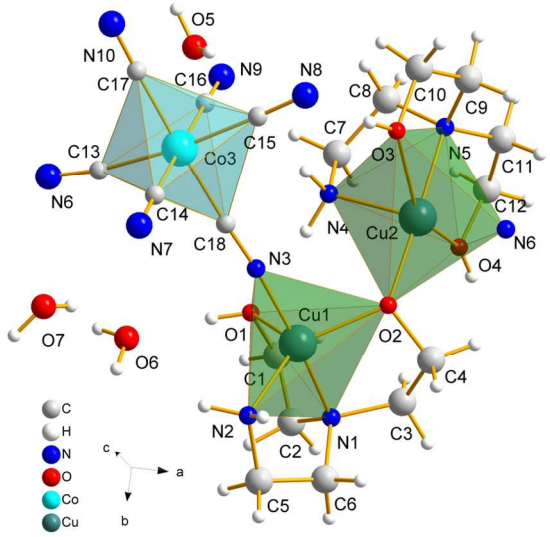

Figure 1. A view of asymmetric Cu1Cu2Co unit of **C2.** Distorted octahedral is drawn as dark green for around $Cu2^{II}$ ion and blue for around $Co3^{III}$.

Table 1. Crystal data and structure refinement of **C2**

Empirical formula	$C_{18}H_{37}N_{10}O_7CoCu_2$
Formula weight / F(000)	691.59 / 1424
Temperature	293(2)
Crystal size (mm)	0.47 x 0.34 x 0.27
Crystal system / space group	Monoclinic / $P2_1/c$
a (Å)	9.2863(4)
b (Å)	20.6105(10)
c (Å)	16.7211(7)
α (°)	90
β (°)	116.179(3)
γ (°)	90
V (Å^3) /Z	2872.0(2) / 4
$Density_{calcd.}$(gcm^{-3})	1.559
Abs. coeff. μ (mm^{-1})	2.092
θ range (°)	1.68-27.32
Index ranges	$-11 \le h \le 11$
	$-25 \le k \le 25$
	$-17 \le l \le 20$
Reflections collected	14715
Independent reflections	4667 [R_{int}=0.0436]
Observed reflections	5606
Data/restrains/parameters	5606/9/373
Final R incides [I ≥2σ(I)]	R_1=0.0304, wR_2=0.0730
R incides (all data)	R_1=0.0419, wR_2=0.0768
Goodness–of-fit on F^2	1.017
Absorption correction, T_{min}/ T_{max}	Integration, 0.4977/0.6313
w=1/[σ^2(Fo^2)+(0.0449P)^2+0.0000P]	P=(Fo^2+2Fc^2)/3
S, $(\Delta/\sigma)_{max}$	1.016/0.002
$\Delta\rho_{max}$, $\Delta\rho_{min}$ (eÅ^{-3})	0.359/-0.403

Results and Discussion

For the synthesis of the studied complexes the "brick and mortar" approach usual way for synthesis coordination compounds was applied. First the appropriate cations (bricks) were prepared and then hexacyanidocobaltate anion was added as a mortar. Single crystals of **C2** were obtained by slow diffusion of ethyl alcohol and water solution. The results of elemental analysis were in good agreement with expected values. The IR spectrum of **C2** contained high number of $\upsilon_{C\equiv N}$ vibrations and thus indicated a different composition structure.

Infrared Spectroscopy (*IR*)

The *IR* spectra of **C1**-**C4** comprise of bands confirming the presence of all the characteristic functional groups in the prepared complexes. The active bands for υ(O-H) and υ(N-H) confirming the presence of *N-bishydeten* ligand fall in the region 3100-3600 cm^{-1} for all complexes. According to the elemental and thermal analysis, it is estimated to be water in these complexes, possibly with the υ(O-H) and υ(N-H) generated in this region with hydrogen bonding (*HB*) interaction is caused to expand. Therefore, the broad stretching bands at 3200-3600 cm^{-1} for the antisymmetric and symmetric υ(O-H) and the sharp bands at 1600-1630 cm^{-1} for δ(O-H) [5,27] indicate the presence of water molecules in the structures of all complexes. The sharp bands at 1616 cm^{-1} (**C1**), 1595 cm^{-1} (**C2**), 1622 cm^{-1} (**C3**) and 1604 cm^{-1} (**C4**) correspond to the uncoordinated and hydrogen bonded water δ(O-H) mode.

The presence of $[Co(CN)_6]^{-3}$ anion in the prepared complexes is proved by υ(C≡N) stretching bands whose positions are an important tool to reveal the number and the type (terminal or bridging) of cyanido groups in the complexes. The υ(C≡N) stretching frequency of the terminal cyanido ligand falls in the range 2000-2100 cm^{-1} while the range 2100-2200 cm^{-1} is characteristic for the cyanido ligand that acts as a bridge or/and the terminal cyanido ligand involved in *HB* interactions [27,28]. The shift of υ(C≡N) to higher wavenumber as compared to that of $K_3[Co(CN)_6]$ is consistent with the formation of cyanido bridge. The *IR* spectra exhibit sharp bands at 2167 and 2124 cm^{-1} for **C1**, 2155 and 2132 cm^{-1} for **C3** and 2157 cm^{-1} for **C4**, while this absorption band at 2129 cm^{-1} occurs for the free $[Co(CN)_6]^{-3}$ [27]. The peaks at 2167, 2155 and 2157 cm^{-1} belong to bridging cyano ligand for **C1**, **C3** and **C4**, respectively and the lower peaks (2124 and 2132 cm^{-1}) can be ascribed to a terminal cyanido group. The spectrum of **C2** is quite different from other complexes, three υ(C≡N) absorption bands at 2167, 2155 and 2157 cm^{-1} were observed and this situation is in agreement with existence of the crystallographically different cyanido groups in its structure. The tentative assignments of the recorded wavenumbers of the structures are given in the experimental section.

Description of the crystal structure of C2

The reaction of Cu^{II}, *N-bishydeten* and $[Co(CN)_6]^{3-}$ resulted in the formation of $[Cu_2(N\text{-}bishydeten)_2Co(CN)_6].3H_2O$, {*catena*-poly [[tetracyanido-1κ^2*C*-μ-cyanido-1:2κ^2*C*:*N*-μ-bis[*N*,*N*-bis(2-hydroxy ethyl)ethylenediamine-2:2'κ^4*N*,*N*',*O*,*O*':O]dicopper^{II} cobaltate^{III}]-μ-cyanido-2:1'κ^2*C*:*N*]trihydrate}. The asymmetric unit of polymeric **C2** consists of one trinuclear -CN-Cu1(*N-bishydeten*)-η-O-Cu2(*N-bishydeten*)-NC-$Co(CN)_4$-CN-{Cu1Cu2Co} unit (Fig. 1) and three water molecules in a *1D* zigzag chain. The $[Cu_2(N\text{-}bishydeten)_2]^{2+}$ cations are linked to the $[Co(CN)_6]^{3-}$ anions via cyanido bridge to give a *1D* neutral coordination polymer chain (Fig. 2). An interesting feature of the structure is that one of two *N-bishydeten* ligand exhibits bridging mode. Through deprotonated η^1-O2 bridge of *N*-

bishydeten, Cu1 and Cu2 are connected to form a binuclear $[Cu_2L_2]$ unit in an interesting manner. The charge of whole

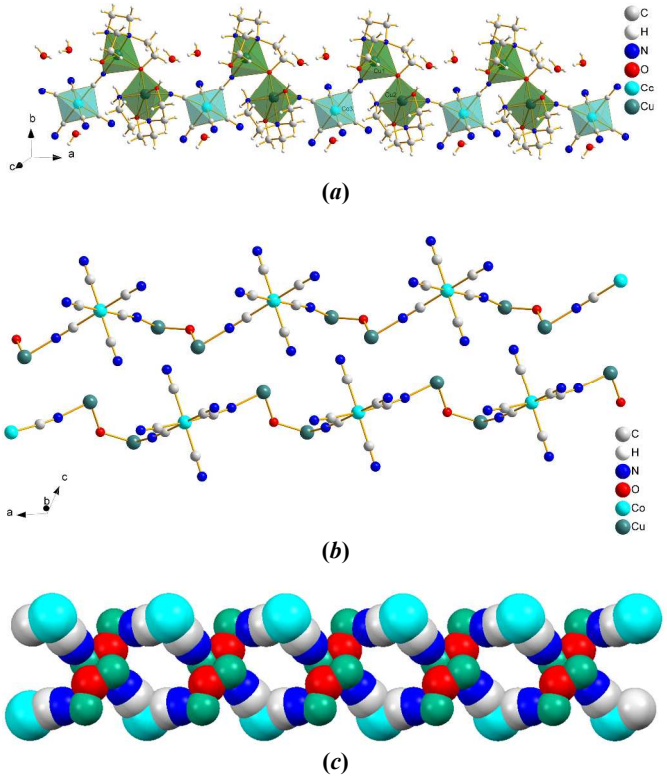

Figure 2. (***a***) *1D* zigzag chain, the chain runs along the [100] direction, (***b***) the backbones of the *2D* chains of **C2** along b axis and (***c***) space filling representation of **C2**. The C, N, H and water molecules are omitted for clarity in (***b***) and (***c***).

structure is counterbalanced by this η^1-O2 deprotonated. The connection manner of *N-bishydeten* in **C2** is similar to that of binuclear cationic complex, $[Zn(OH)(\mu\text{-}(N\text{-}bishydeten\text{-}H)Zn(N\text{-}bishydeten)]^{2+}$, synthesized by Song et. al [23]. In the literature there are examples consisting two Cu^{II} ions with five or six coordination and these Cu^{II} ions are linked with two alkoxo oxygens to each other [20,29,30]. The most important feature of **C2** structure is the connection with the η^1-O2 between the Cu1 and Cu2. The Cu1 and Cu2 atoms in **C2** are penta- and hexa-coordinated, respectively and the coordination number five and six for Cu^{II} are very common. [3,5,6,10,12,14,17,18,20]. But **C2** has Cu^{II} ions having both five and six coordinations reported for the first time in the literature as far as we know.

The Cu1 is five coordinated in a N_3O_2 environment; formed by two pairs of *N*- and *O*- from *N-bishydeten* and one *N*- from bridging cyanido. In order to describe the geometry of the metal environment, Addison τ parameter is used. τ parameter determines the percentage of trigonal distortion from square pyramidal geometry. This parameter is defined as $\tau = \theta - \Phi/60$, where θ and Φ are the two largest coordination angles. The τ parameter is 0 for an ideal square pyramidal geometry, while τ is 1 for the perfectly trigonal bipyramidal geometry [31]. For **C2** the Cu1 adopts a distorted trigonal bipyramidal stereochemistry with a τ value of 0.52. In this geometry, NH_2-, *O*- and η^1-*O* donor atoms of *N-bishydeten* form equatorial plane while bridging cyanido group provided by $[Co(CN)_6]^{3-}$ and tertiary *N*- atom of the ligand occupy axial positions. The distortion from the ideal trigonal bipyramidal geometry is evident from the fact that the axial N1-Cu1-N3 angle of 171.38(10)° which is significantly bent from linearity and the equatorial angles varing from 102.27(8)° to 140.00(9)° (Fig. 3). The *N-bishydeten* is subject to structural disorder. The Cu1-O2

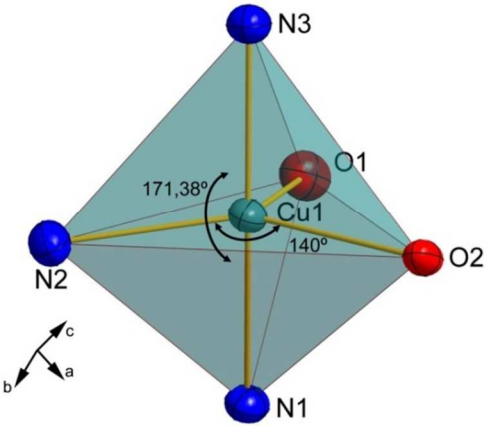

Figure 3. The environment distorted trigonal bipyramidal of Cu1. All atoms except for the Cu1-coordinated atoms have been omitted for the clarity.

(1.984(16) Å) bond distance is shorter than that of Cu1-O1 (2.292(2) Å). And the Cu1-N distances are in the range 1.951(2)-2.032(2) Å. Bond lengths in the coordination environment of the Cu1 follow the O1 > N2 > N1 > O2 > N3 order. While the tension resulting from methylene groups of *N-bishydeten* causes expansion of N2-Cu1-N3 (96.31(9) °) and O2-Cu1-N3 (97.24(8) °) angles, the same tension narrows N1-Cu1-O1 (80.84(9) °), N2-Cu1-N1 (85.42(9) °) and N1-Cu1-O2 (86.67(8) °) angles regarding ideal value. On the other hand, the linearity of N1-Cu1-N3 at the axial position bent with a 171.38(10) °. The Cu1-N3-C18 angle of 169.5(2)° is in a bent fashion, whereas the Co3-C18-N3 angle of 177.1(1)° is close to linearity as can be seen in Table 2.

Table 2. Selected geometric parameters of **C2** (Å, °)

Bond distances (Å)			
Cu1-N1	2.007(2)	Co3-C13	1.891(3)
Cu1-N2	2.032(2)	Co3-C14	1.891(3)
Cu1-N3	1.951(2)	Co3-C15	1.885(3)
Cu1-O1	2.292(2)	Co3-C16	1.903(3)
Cu1-O2	1.984(16)	Co3-C17	1.892(3)
Cu2-N4	1.980(2)	Co3-C18	1.891(2)
Cu2-N5	2.100(2)	C13-N6	1.146(3)
Cu2-N6	1.973(2)	C14-N7	1.151(4)
Cu2-O2	1.981(17)	C15-N8	1.150(3)
Cu2-O3	2.502(2)	C16-N9	1.146(4)
Cu2-O4	2.488(2)	C17-N10	1.140(3)
		C18-N3	1.145(3)
Bond angles (°)			
Co3-C13-N6	172.4(2)	O2-Cu1-N2	140.00(9)
Co3-C14-N7	178.3(3)	O2-Cu1-O1	102.27(8)
Co3-C15-N8	177.3(3)	N1-Cu1-N2	85.42(9)
Co3-C16-N9	178.5(2)	N1-Cu1-O1	80.84(9)
Co3-C17-N10	178.6(2)	N2-Cu1-O1	114.98(9)
Co3-C18-N3	177.1(2)	N3-Cu1-O1	90.80(9)
C15-Co3-C13	174.15(10)	N3-Cu1-N2	96.31(9)
C14-Co3-C16	178.10(11)	N3-Cu1-O2	97.24(8)
C18-Co3-C17	177.79(11)	N3-Cu1-N1	171.38(10)
C15-Co3-C18	90.49(10)	O2-Cu2-O3	109.74(8)
C13-Co3-C18	94.66(10)	O2-Cu2-O4	101.14(8)
C14-Co3-C18	89.23(11)	O2-Cu2-N5	174.58(8)
C15-Co3-C17	87.36(11)	O3-Cu2-O4	149.12(9)

C13-Co3-C17	87.51(10)	N4-Cu2-N5	83.03(9)
C14-Co3-C17	90.34(12)	N4-Cu2-O2	93.53(8)
C13-Co3-C14	91.08(11)	N4-Cu2-O2	93.53(9)
C15-Co3-C16	89.05(11)	N4-Cu2-O3	86.1(1)
C13-Co3-C16	88.28(11)	N4-Cu2-O4	91.9(1)
C15-Co3-C14	91.76(12)	N5-Cu2-O4	74.86(9)
C18-Co3-C16	89.04(11)	N5-Cu2-O3	74.31(9)
C17-Co3-C16	91.42(11)	N6-Cu2-N5	92.76(9)
Cu2-N6-C13	166.5(2)	N6-Cu2-O3	87.00(1)
Cu1-N3-C18	169.5(2)	N6-Cu2-O4	92.82(1)
Cu2 O2 Cu1	130.36(9)	N6-Cu2-N4	172.70(9)
O2-Cu1-N1	86.67(8)	N6-Cu2-O2	91.09(8)

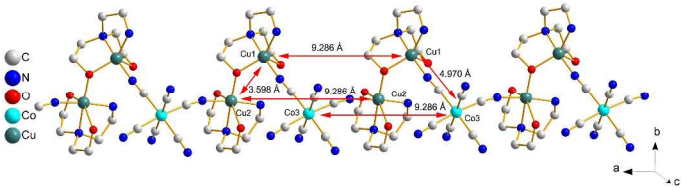

Figure 4. The adjacent Co3-Cu1, Cu1-Cu2 and Cu2-Co3 distances in **C2**. H atoms and water molecules are omitted for clarity.

The Cu2 is six-coordinated with tetradentate (N4, N5, O3 and O4) *N-bishydeten*, one *N*- atom from bridging cyanido form $[Co(CN)_6]^{3-}$ and η^1-O2. The geometry around Cu2 is a distorted (elongated) octahedral with short bonds at the equatorial positions [1.980(2)-2.100(2) Å] and long bonds formed by two *O*- atoms from *N-bishydeten* at the axial positions [Cu2-O3 2.502(2) Å; Cu2-O4 2.488(2) Å]. The observation of short equatorial and long axial bonds for an octahedral coordination is as expected for the Cu^{II} having d^9 electron configuration due to the *Jahn-Teller* distortion. The degree of tetragonal *Jahn-Teller* distortion of the Cu2 site is T = 0.805 (T is the ratio of mean in-plane Cu2-X bond lengths to mean axial Cu2-X bond lengths) [32]. The notably deviations of O-Cu2-N, O-Cu2-O and N-Cu2-N bond angles from the 90° and 180°, which are presumably the result of the steric constraints arising from the shape of the ligand, are an evidence of distorted octahedral structure. On the other hand, in $Cu2N_3O_3$, Cu2-N5 is the longest bond distantance of the equatorial plane because of steric hindrance and the tension of methylene groups of *N-bishydeten*, probably. Also the same reason causes narrowing of the N4-Cu2-N5, O3-Cu2-N5 and O4-Cu2-N5 angles regarding ideal value. The different *HB* interactions of O3 and O4 in **C2** lead to a small difference between the Cu2-O3 and Cu2-O4 bond lengths.

The Cu-N bond distances around Cu1 and Cu2 are very similar to $[C_{38}H_{38}CoCu_2N_{14}O]^+[C_{22}H_{18}CoCuN_{10}]^-.7H_2O$ [3], $[Cu(dmpn)_2]_3[Co(CN)_6]_2.12H_2O$ and $[Cu(dmpn)_2]_2[Co(CN)_6].ClO_4.3H_2O$ [5], $[\{(Cu(dien))Co(CN)_6\}_n[Cu(dien)(H_2O)Co(CN)_6]_n.5nH_2O$ [10], $\{[Cu(en)_2][KCo(CN)_6]\}_n$ [11], $[Cu(C_4H_{12}N_2)_2]_3[Co(CN)_6].4H_2O$ [12], [Cu(*N-bishydeten*)$_2$][Ni(CN)$_4$] [21], [Cu(*N-bishydeten*)$_2$][Pd(CN)$_4$] and [Cu(*N-bishydeten*)Pd(CN)$_4$] [22] and [Cu(*N-bishydeten*)Pt(CN)$_4$] [33] complexes reported in the literature. The Cu1 and Cu2 bond distances with the deprotonated η^1-O2 bridge are similar, which may be caused by the absence of any free group at positions of O2 atom. The Cu1-O-Cu2 bond angle (130.36 °) shows a quite large deviation from linearity because of steric hindrance of *N-bishydeten* ligand which η^1-O2 atom is belonged to.

$[Co(CN)_6]^{3-}$ anion linking two cationic units by cyanido bridges has an usual six coordinated octahedral arrangement, with slight distortions as indicated by variation of the *cis* angles [87.36(11)-94.66(10)°] and *trans* angles [174.15(10)-178.10(11)°] from the ideal value of 90° and 180°, respectively (see Table 2). The Co(3)-C and C-N distances are grouped together ranging from 1.885-1.903 Å and 1.140-1.151 Å, respectively. Co3 central metal is almost at the same distance from Cu1 and Cu2. Three crystallographically distinct cyanido groups show different connections via their *N* atoms and the angles formed by bridging cyanido groups (Co3-C18-N3 and Co3-C13-N6) are bent more than that of the terminal ones. All the bond

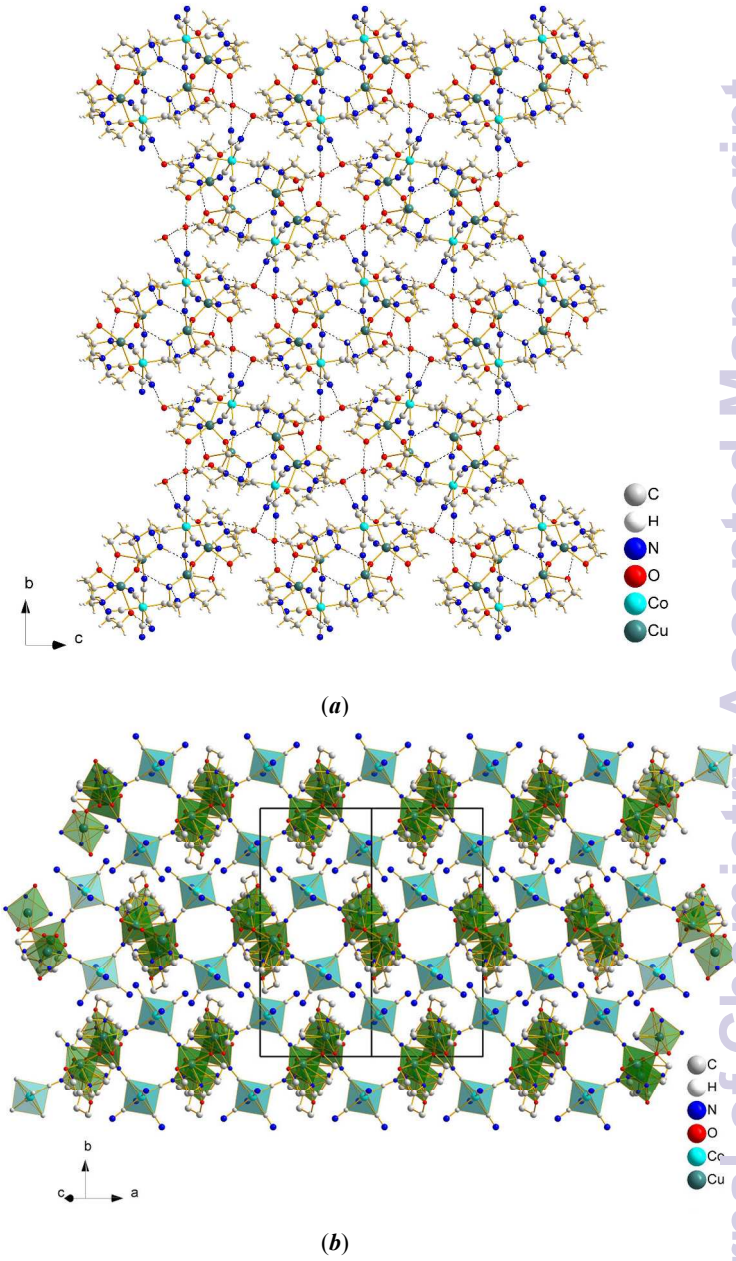

Figure 5. (***a***) *HB* networks and (***b***) packing diagram of **C2** along b axis where free water molecules were omitted.

distances and angles around Co3 compare well with the corresponding values in the cyanido-bridged Cu^{II}-Co^{III} bimetallic assemblies [2,5,6,10,12,14,17,18].

The adjacent Co3-Cu1, Cu1-Cu2 and Cu2-Co3 distances are 4.970(5) Å, 3.598(4) and Å 4.943(6) Å, respectively. The nearest Cu1-Cu1, Cu2-Cu2 and Co3-Co3 are at the same value of 9.286 Å (Fig. 4).

HBs are important and effective tool in forming a layered structure in the intermolecular network of the crystal lattices of this type of

compounds (Fig. 5). The details of all *HBs* of **C2** are given in Table 3. *N*- atoms from three of the four terminal cyanido ligand form *HBs* to the uncoordinated water molecules (O5, O6 and O7) and the water molecules also have *HBs* interactions with each other. The NH_2-groups of two *N-bishydeten* form *HBs* with *OH-* and terminal cyanido groups. These bandings impart overall stability of the system. The N-H···N type *HBs* has an accepted bond length of 3.38 Å, which is the upper limit for an N···N distance [34,35]. In **C2**, N2-H2D···N7 interaction (3.29(4) Å) is shorter than 3.38 Å, while the N4-H4D···N9 interaction (3.32(3) Å) is similar to the upper limit and to the sum of the van der Waals radii of N···N (3.10 Å).

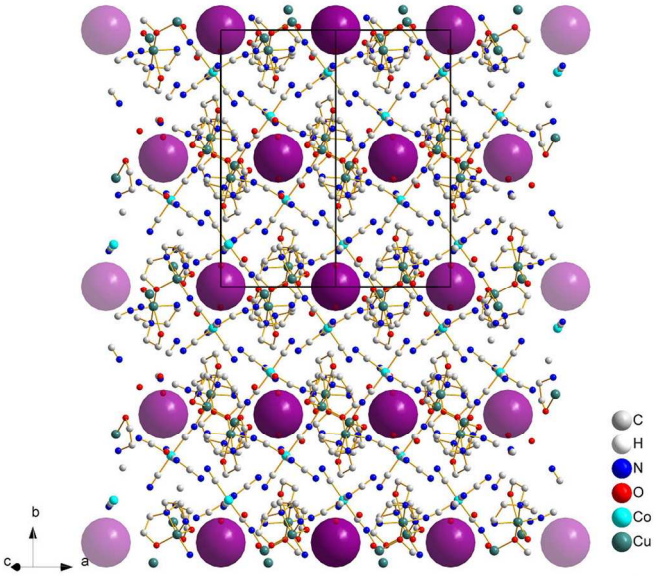

(***a***)

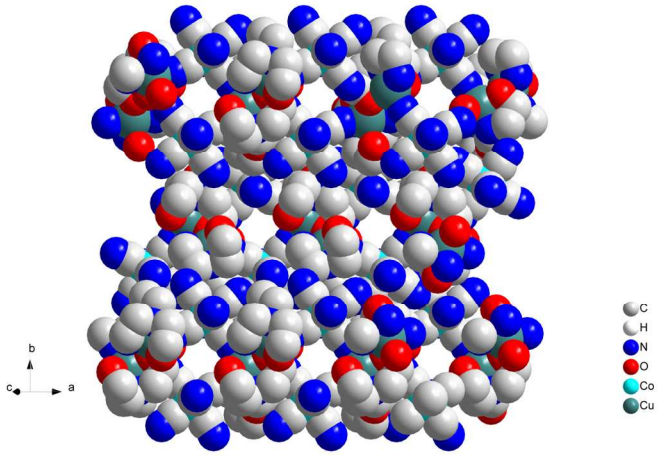

(***b***)

Figure 6. (***a***)The cavities of *3D* supramolecular framework of **C2** (Purple spheres represent the cavities. Hydrogen atoms have been omitted for clarity) and (***b***) Space filling representation of **C2**. Water molecules have been omitted clarity.

Table 3. Hydrogen bonds (Å, °) for **C2**

D-H···A	*d(D–H)*	*d(H···A)*	*d(D···A)*	*<(DHA)*	*Symmetry codes**
N2-H2C···O2	0.90	2.33	3.230(3)	175	1-x,-y,-z
N2-H2D···N7	0.90	2.52	3.29(4)	144	-x,-y,-z
N4-H4C···O1	0.90	2.00	2.90(3)	175	-
N4-H4D···N9	0.90	2.56	3.32(3)	142	-
O1-H1E···O6	0.80(4)	1.76(4)	2.56(3)	174(5)	1-x,-1/2+y, 1/2-z
O3-H3E···N8	0.80(4)	2.20(4)	2.99(4)	173(4)	-
O4-H4E···O7	0.77(4)	1.97(4)	2.73(3)	171(4)	2-x,-y,1-z
O5-H5C···N9	0.85(19)	2.08(2)	2.91(4)	165(5)	-
O5-H5D···N8	0.85(19)	2.04(2)	2.87(3)	171(5)	x,1/2-y,1/2+z
O6-H6C···O7	0.82(18)	1.93(19)	2.75(4)	172(5)	x,1/2-y,-1/2+z
O6-H6D···N7	0.83(19)	1.98(19)	2.81(4)	174(6)	1+x,1/2-y,1/2+ z
O7-H7C···N10	0.84(17)	1.94(19)	2.78(3)	174(4)	1+x,1/2-y,1/2+ z
O7-H7D···O5	0.84(18)	1.87(2)	2.70(3)	170(4)	-

The neighboring *1D* polymeric chains are further stacked to form a *3D* supramolecular framework via all above mentioned *HBs* interactions between the $[Co(CN)_6]^{3-}$ anions and free water molecules. The packing of titled complex are encapsulated in the interblended cavities of such *3D* supramolecular framework. The cavities are occupied by the free water molecules (Fig. 6). Nevertheless, there still remains an unoccupied solvent accessible void of 148.3 $Å^3$ (% 5.2 of the unit cell volume).

Thermal Analysis

The thermal decomposition behaviors of **C1-C4** were studied in the temperature range 35-1130 °C in the flowing atmosphere of N_2. Thermal decomposition of **C1** proceeds in five stages. In the first stage, **C1** starts to lose three water molecules between 38 and 110 °C (found. 8.71%, calcd. 7.92%). After this temperature the anhydrous **C1** is stable up to 237 °C and beyond this temperature, it decomposes and this mass loss exactly corresponds exactly to one *N-bishydeten* molecule (found. 21.06%, calcd. 21.73%). The mass loss in the temperature range 334-499 °C corresponds to the other ligand molecule and three cyanido groups (found. 32.44%, calcd. 33.18%). The remaining cyanido groups are released between 499 and 567 °C (found. 10.82%, calcd. 11.45%).

The thermal analysis of **C2** was performed with a heating rate of 3 $^oCmin^{-1}$. The **C2** was decomposed in seven-step process. The dehydration process takes place with a mass loss of 8.51% in the first two stages in the temperature ranges of 35-114 °C (calcd. 7.81%). Then, two *N-bishydeten* molecules are released (114-372 °C) in the following four stages consecutively (found. 40.52%, calcd. 40.54%). In the last stage, six cyanido groups are decomposed between 372 and 513 °C (found. 22.17%, calcd. 22.57%).

Thermal decomposition of **C3** proceeds in six stage. The first stage completing at 150 °C with a mass loss of 12.03% is attributed to the loss of five water molecules (calcd. 12.31%). In the following three stages (150 and 645 °C) the mass loss of 40.32% is observed due to the successive decomposition of two *N-bishydeten* (calcd. 40.53%). In the 645-857 °C temperature range, weight loss of 21.24% involves the decomposition of cyanido groups (calc. 21.35%). Lastly, the exothermic stage (857 and 914 °C) is due to the vaporization of 12.5% of all Zn atoms (found. 4.68%, calcd. 4.47). All Zn is not liberated from structure in spite of the fact that boiling point of Zn is 907 °C but. This situation is thought to arise from the formation of

ZnO having high thermal stability with a high decomposition enthalpy (-9608J/g) at the last stage [36].
The stages with the temperature range of 159-454 ^{o}C are related to the successive decompositions of water molecules and one *N-bishydeten* in thermal analysis of **C4** (found. 33.78%, calcd. 32.34%). This stage is followed by the release of potassium and four cyanido groups at 576 ^{o}C (found. 25.83%, calcd. 26.43%). The remaining cyanido groups and 0.25% Cd are liberated from the structure (found. 14.13%, calcd. 14.79%). In the temperature range of 792-854 ^{o}C the mass increase with 2.89% is attributed to the formation of CdO. CdO amorphous structure decomposed in the range of 900-1000 ^{o}C. According to this knowledge CdO decomposed in the temperature range of 895-1137 ^{o}C (found. 15.49%, calcd. 15.56%) and the final product is Co.

EPR and Magnetic susceptibility studies

EPR spectrum for **C1** could not be observed due to short relaxation times or the large zero-field splitting of the Ni^{II} ions at room temperature. Figure 7 shows the powder *EPR* spectrum of **C2** at room temperature. Parallel and perpendicular two components have been observed in this spectrum. Hyperfine splitting could not be resolved due to line broadening originated from spin-orbital and spin-exchange interactions because of the excess spin concentration. The values of $g_{//}$ and $g_{\perp}$ components were extracted from the powder spectrum. The principal values of these are the following: $g_{//}$= 2.242, $g_{\perp}$= 2.068. The g parameters have indicated that the paramagnetic center is axially symmetric. These spectrum belong to Cu^{2+} ion (S = 1/2, I = 3/2). From the order of $g_{//}>g_{\perp}>ge$ (free electron g value, g_e = 2.0023), it can be concluded that $Cu2^{II}$ ion is located in tetragonal distorted octahedral sites (D_{4h}) elongated along the z-axis and the ground state of the paramagnetic electron is $d_{x^2-y^2}$ ($^2B_{1g}$ state) [37-40]. The result obtained from *EPR* is confirmed by the single crystal analysis data of **C2** (Table 2). On the other hand, due to that the surrounding of $Cu1^{II}$ is disordered triangular bipyramid (Fig. 3), the single electron in $Cu1^{II}$ is expected to be in d_z^2 orbital. In this case $g_{\perp}$ should be bigger than $g_{//}$. Despite this, we could not observe such a line hierarchy in the EPR spectrum. The reason might be as following: The $Cu1^{II}$ surrounding is an intermediate between a square pyramid and a trigonal bipyramid since τ = 0.52,, by deviating considerably from ideal triangular bipyramidal structure, which is supported with the X-ray data. So there could be the increased mixing of $d_{x^2-y^2}$ character into d_z^2 orbital by vibronic interaction. Thus, the peaks belonging to environments of both Cu^{II} ions can be overlapping, and collapse to peaks observed. Such a behavior is similar to those of some reported binuclear copper complexes [41,42].
The magnetic susceptibility of **C1** was obtained in the temperature range of 10-300 K. The temperature dependence of the molar magnetic susceptibility (χ_m) and χ_mT are shown in Fig. 8. For **C1**, the temperature dependence of χ_m was fitted by relation of $\alpha + C/(T-\theta)$, where α is temperature independent susceptibility (TIP) [43].

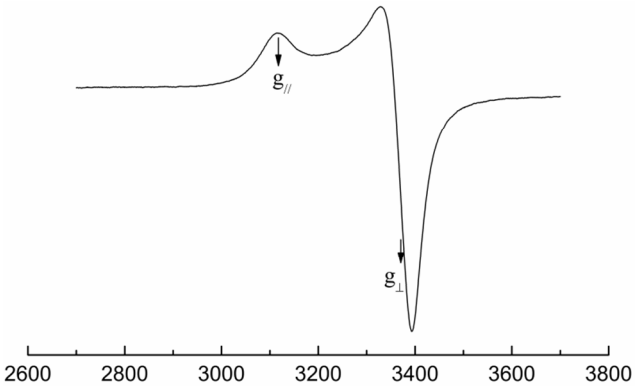

Figure 7. The powder *EPR* spectrum of **C2** at room temperature.

Determined fitting results: $C = 2.263 \pm 0.0003\ emuK/mol.Oe$, $\alpha = 0.00115 \pm 0.000002\ emu/mol.Oe$ and $\theta = -0.775 \pm 0.002\ K$. The TIP can originate from the fact the ground state couples with excited states due to the orbital moments of *d* electrons or Pauli paramagnetism is associated with parallel alignment tendency of magnetic dipoles of free electrons in metals to the applied magnetic field. The effective magnetic moment for **C1**, μ_{eff}, was calculated to be 4.257 in Bohr magneton (μ_B), using the relation $2.83(\chi_m T)^{1/2}$.
Below 10K, for **C1** there might be a very small antiferromagnetic interaction in the structure, as seen from knee down in the inset of Fig. 8. This magnetic interaction might be between and within the chains through *CN* bridges and *HBs*.

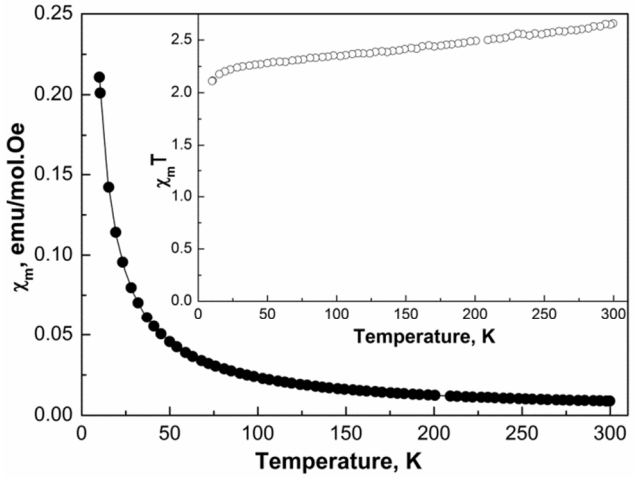

Figure 8. The temperature dependence of the molar magnetic susceptibility χ_m for **C1**. Solid line represents a fit by the Curie–Weiss law. Inset: The temperature dependence of χ_mT.

The values of molar magnetic susceptibility for the **C2** having dimeric copper units were measured in the temperature range of 10-300 K. The temperature dependence of the molar magnetic susceptibility (χ_m) and χ_mT for **C2** is shown in Fig. 9. As the temperature decreases, the value of the χ_m increases continuously, reaches a maximum around 113 K and then falls to a minimum at 25 K. This kind of magnetic behaviour for **C2** shows the presence of strong antiferromagnetic interaction between two oxygen-bridged Cu^{II} ions. The rapid rise of χ_m below 25 K is due to small amounts of paramagnetic impurities such as Cu^{II}. The solid line in Fig. 8 represents a fit to the equation 1 (Van Vleck equation for $S_1 = S_2 =$

1/2) derived from the eigenvalues of $H = -2JS_1S_2$ known as Heisenberg-Dirac-Van Vleck (HDVV) Hamiltonian for the exchanged coupled two equivalent spin centers [44-46].

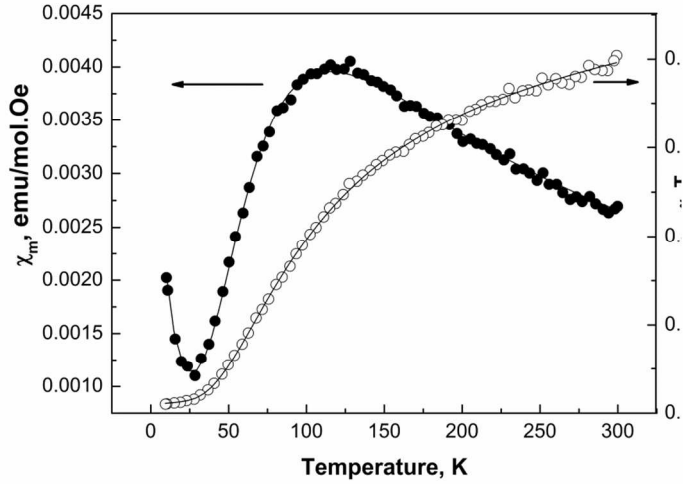

Figure 9. The temperature dependence of the molar magnetic susceptibility χ_m and χ_mT for **C2**. Solid line represents the fitted function.

$$\chi_m = (1-p)\frac{N_A g^2\beta^2(2e^{2J/k_BT})}{k_BT(1+3e^{2J/k_BT})} + p\frac{N_A g^2\beta^2}{2k_BT} + \alpha \qquad \text{Eq. (1)}$$

The symbols in equation 1 have the usual meanings. p is the molar fraction of paramagnetic impurity. From an excellent fit of magnetic data to equation 1, the magnetic parameters were determined as 2J = - 131 ± 1 cm^{-1}, g = 2.102 ± 0.001, p = 0.011 ± 0.00002 and α = 0.00034 ± 0.000001 emu/mol.Oe. These values are consistent with those of the literature [47-53]. The effective magnetic moment at room temperature, μ_{eff}, was calculated to be 2.54 in Bohr magneton (μ_B). From these results, we conclude that there exists a strong antiferromagnetic super-exchange interaction, through the bridging oxygen between Cu^{II} ions of binuclear **C2.** A similar interaction was also observed for the other complexes in the literature [54].

Conclusions

In this work four new heterometallic cyanido complexes, $[Ni_2(N\text{-}bishydeten)_2Co(CN)_6].3H_2O$ (**C1**), $[Cu_2(N\text{-}bishydeten)_2Co(CN)_6].3H_2O$ (**C2**), $[Zn_2(N\text{-}bishydeten)_2Co(CN)_6].5H_2O$ (**C3**) and $K[Cd(N\text{-}bishydeten)Co(CN)_6].1.5H_2O$ (**C4**), were prepared and characterized by vibrational spectroscopy, thermal and elemental analysis techniques. The polymeric structure of **C2** was determined by the X-ray single crystal method. This method reveals that *N-bishydeten* acts as a tetradentate ligand (NH_2-, *N-* , *O-* and *O-*) and one of two *N-bishydeten* bridged Cu1 and Cu2 through η^1-O2. This η^1-O2 is deprotonated and counterbalanced the charge of **C2**. The most important feature of **C2** structure is the connection with the η^1-O2 between the Cu1 and Cu2, which is seen for the first time in the literature. In this structure, the Co^{III} ions are six coordinated to six carbon atoms from cyanido groups. On the other hand, two nitrogen atoms are coordinated to Cu1 and Cu2 atoms. The Cu1 adopts a distorted trigonal bipyramidal stereochemistry, having a τ value of 52. And the Cu2 adopts a distorted octahedral geometry with a value of T = 0.805 Jahn-Teller distortion. The *IR* spectrum of **C2** is quite different from other complexes, three υ(C≡N) absorption bands were observed due to different cyanido groups in its structure. The thermal decomposition of **C1-C4** in N_2 was studied using TG/DTG/DTA analysis. Magnetic study of **C1**, reveals a very small antiferromagnetic interaction below 10K through *CN* bridges and *HBs*. And **C2** reveals a strong antiferromagnetic exchange interaction between oxygen-bridged two Cu^{II} ions.

Acknowledgements

The authors thank the Scientific and Technical Research Council of Turkey (TUBİTAK, Grant TBAG-104T205) and the Gaziosmanpaşa University Research Foundation (Grant 2010/110) for financial support.

Notes and references

[a] *Bioengineering Department, Engineering Faculty, Tunceli University, 62100, Tunceli, TURKEY. Fax: +90(428)2131624; Tel:+90(428)2131752; Şengül Aslan Korkmaz: sengul482@gmail.com; saslankorkmaz@tunceli.edu.tr*
[b] *Department of Chemistry, Art and Science Faculty, Gaziosmanpaşa University, 60400, Tokat, TURKEY. Fax: +90(356)2521585; Tel: +90(356)2521616; Ahmet Karadağ: ahmet.karadag@gop.edu.tr; akaradag68@gmail.com*
[c] *Department of Physics, Art and Science Faculty, Yıldız Technical University, 34220, İstanbul, TURKEY. Fax: +90(212)3834234; Tel: +90(212)3834254; Yusuf Yerli: yyerli@yildiz.edu.tr*
[d] *Department of Physics, Art and Science Faculty, Giresun University, 28200, Giresun, TURKEY. Fax: +90(454)3101477; Tel: +90(454)3101400; Serkan Soylu; serkan.soylu@giresun.edu.tr*

†Electronic Supplementary Information (ESI) available: CCDC ID: 983075 contains the crystallographic data for **C2**. These data can be obtained free charge of via https://www.ccdc.cam.ac.uk/services/structure_deposit/ or from the Cambridge Crystallographic Data Centre, 12 Union Road, Cambridge CB2 1EZ, UK; fax: (+44) 1223-336-033 or e-mail: deposit@ccdc.cam.ac.uk. See DOI: 10.1039/b000000x/

References

1 S.R. Batten, S.M. Neville, D.R. Turner, Coordination Polymers Design, Analysis and Application, (RSC, Cambridge, UK, 2009), p. 221.
2 F.H.O. Ishiruji, N.L. Speziali, M.G.F. Vaz, F.S. Nunes, J. Braz. Chem. Soc., 2010, **21**, **7**, 1195 (and references therein).
3 C.R. Choudhury, S.K. Dey, S. Mitra, N. Mondal, J. Ribas, K.M. Abdul Malik, Bull. Chem. Soc. Jpn., 2004, **77**, 959.
4 M. Ohba, N. Usuki, N. Fukita, H. Ōhkawa, Inorg. Chem., 1998, **37**, 3349.
5 N. Mondal, D.K. Dey, S. Mitra, V. Gramlich, Polyhedron, 2001, **20**, 607.
6 Y.P. Li, P. Yang, Z.X. Huang, F.X. Xie, Acta Cryst., 2005, **C61**, m122.
7 W.W. Sima, W. Zhang, Inorg. Chem. Commun., 2011, **14**, 176.
8 D.M. Gil, R.E. Carbonio, M. I. Gómez, J. Mol. Struct., 2013, **1041**, 23.
9 D. Karaağaç, G.S. Kürkçüoğlu, O.Z. Yeşilel, M. Taş, Polyhedron, 2013, **62**, 286.
10 M. Ferbinteanu, S. Tanase, M. Andruha, Y. Journaux, F. Cimpoesu, I. Strenger, E. Riviére, Polyhedron, 1999, **18**, 3019.
11 C. Xie, W. Wanga, J.Z. Zoua, H.L. Liua, X.P. Shenb, B.L. Lib, H.M. Huc, Z. Xu, J. Coord. Chem., 2004, **57**, **17-18**, 1519.
12 T. Akitsu, Y. Einaga, Acta Cryst., 2006, **E62**, m750.

13 G. Li, O. Sato, T. Akitsu, Y. Einaga, Journal of Solid State Chemistry, 2004, **177**, 3835.
14 B. Li, X. Shen, K. Yu, Z. Xu, J. Coord. Chem., 2002, **55**, **10**, 1191.
15 M.K. Saha, F. Lloret, I. Bernal, Inorg. Chem., 2004, 43, 1969.
16 S. Perruchas, K. Boubekeur, P. Molinié, Polyhedron, 2005, **24**, 1555.
17 B. Samanta, J. Chakraborty, R.K.B. Singh, M.K. Saha, S.R. Batten, P. Jensen, M.S.E. Fallah, S. Mitra, Polyhedron, 2007, **26**, 4354.
18 S.Z. Zhan, D.S. Sun, J.G. Wang, J.Y. Zhou, A.Q. Liang, J.Y. Su, J. Coord. Chem., 2008, **61**, 550.
19 M. Atanasov, C. Busche, P. Comba, F. El Hallak, B. Martin, G. Rajaraman, J. van Slageren, H. Wadepohl, Inorg. Chem., 2008, **47**, 8112.
20 J. Xia, T.T. Li, X.Q. Zhao, J.F. Wei, J Coord. Chem., 2013, **66**, **4**, 539.
21 A. Karadağ, Ş. Aslan Korkmaz, Ö. Andaç, Y. Yerli, Y. Topcu, J Coord. Chem., 2012, **65**, 1685.
22 Ş. Aslan Korkmaz, A. Karadağ, N. Korkmaz, Ö. Andaç, N. Gürbüz, İ. Özdemir, R. Topkaya, J. Coord. Chem., 2013, **66**, **17**, 3072.
23 B. Song, J. Reuber, C. Ochs, F.E. Hahn, T. Lügger, C. Orvig, Inorg. Chem., 2001, **40**, 1527.
24 U. Asseline, M. Chassignol, J. Draus, M. Durand, J. Maurizot, Bioorganic & Medicinal Chemistry, 2003, **11**, 3499.
25 Stoe & Cie. X-Area Version 1.18 and X-Red32 Version 1.04, (Stoe & Cie, Darmstadt, Germany, 2002)
26 G.H. Sheldrick, SHELXS-97 and SHELXL-97 (Gottingen University, Germany, 1997)
27 K. Nakamoto, Infrared and Raman spectra of inorganic and coordination compounds (John Wiley and Sons, Inc., New York, 1978), p. 259
28 S. Tanase, J. Reedijk, Coord. Chem. Rev., 2006, **250**, 2501.
29 P.S. Mukherjeee, T.K. Maji, T. Mallah, E. Zangrando, L. Randaccio, N.R. Chaudhuri, Inorg. Chim. Acta, 2001, **315**, 249.
30 R.B. Samulewski, J.C. Rocha, R. Stieler, E.S. Lang, D.J. Evans, G. Poneti, O.R. Nascimento, R.R. Ribeiro, F.S. Nunes, Polyhedron, 2011, **30**, 1997.
31 A.W. Addison, T.N. Rao, J. Reedijk, J.V. Rijn, G.C. Verschoor, J. Chem. Soc., Dalton Trans., 1984, **27**, 1349.
32 R.J. Dudley, B.J. Hathaway, J. Chem. Soc. A., 1970, **12**, 2799.
33 Ş. Aslan Korkmaz, Supervisor: A. Karadağ, Ph. D. Thesis, Gaziosmanpaşa Unv., Tokat, Türkiye, 2013.
34 A. Karadağ, A. Şenocak, Y. Yerli, E. Şahin, R. Topkaya, J. Inorg. Organomet. Polym., 2012, **22**, 369.
35 G.A. Jeffrey, W. Saenger, Hydrogen bonding in biological structures (Springer, Berlin, 1991)
36 A. Şenocak A. Karadağ, E. Şahin, Y. Yerli, J. Inorg. Organomet. Polym., 2011, **21**, 438.
37 R.J. Dudley and B.J. Hathaway, J. Chem. Soc. A, 1970, **12**, 2799.
38 E.Di. Mauro, S.M. Domiciano, J. Phys. Chem. Solids, 1999 **60**, 1849.
39 Y. Yerli, S. Kazan, O. Yalçın, B. Aktas¸ Spectrochimica Acta Part A, 2006, **64**, 642.
40 Y. Yerli , F. Köksal, A. Karadag, Solid State Sciences, 2003, **5**, 1319.
41 A. Banerjee, S. Sarkar, D. Chopra, E. Colacio, K. K. Rajak, Inorg. Chem. 2008, **47**, 4023.
42 B.-M. Kukovec, Z. Popovic, B. Kozlevcar, Z. Jaglicic, Polyhedron, 2008, **27**, 3631.
43 J.J. Earney, C.P.B. Finn, B.M. Najafabadi, J. Phys. C: Solid St. Phys., 1971, **4**, 1013.
44 W. Heisenberg, Z. Phys., 1926, **38**, 411.
45 P.A.M. Dirac, Proc. R. Soc. London, Ser A, 1929, **123**, 714.
46 J.H. Van Vleck, Theory of Electrical and Magnetic Susceptibrlities (Oxford University Press, Oxford, 1932)
47 M.G. lvareza, G. Alzueta, J. Borra´sa, S.G. Grandab, J.M. Montejo-Bernardo, J. Inorg. Biochem., 2003, **96**, 443.
48 M. Leluk, B. Jegowska-Trzebiatowska, J. Jezierska, Polyhedron, 1991, **10**, 1653.
49 S. Youngme, A. Cheansirisomboon, C. Danvirutai, C. Pakawatchaib, N. Chaichit, C. Engkagul, G.A. van Albada, J.S. Costa, J. Reedijk, Polyhedron, 2008, **27**, 1875.
50 M.L. Tonnet, S. Yamada, I.G. Ross, Trans. Faraday Soc., 1964, **60**, 840.
51 R. Cejudo-Marin, G. Alzuet, S. Ferrer, J. Borras, A. Castineiras, E. Monzani, L. Casella, Inorg. Chem., 2004, **43**, 6805.
52 M.S. Palacios, J.M. Dance, Polyhedron, 1988, **7**, 543.
53 L. Gutierrez, G. Alzuet, J. Borras, A. Castineiras, A. Rodrıguez-Fortea, E. Ruiz, Inorg. Chem., 2001, **40**, 3089.
54 N. A. Rey, A. Neves, A. J. Bortoluzzi, W. Haasec, Z. Tomkowicz, Dalton Trans., 2012, **41**, 7196.